

## Synthesis of Heterometal Cluster Complexes by the Reaction of Cobaltadichalcogenolato Complexes with Groups 6 and 8 Metal Carbonyls

Masaki Murata, Satoru Habe, Shingo Araki, Kosuke Namiki, Teppei Yamada, Norikiyo Nakagawa, Takuya Nankawa, Masayuki Nihei, Jun Mizutani, Masato Kurihara, and Hiroshi Nishihara\*

Department of Chemistry, School of Science, The University of Tokyo, Hongo, Bunkyo-ku, Tokyo 113-0033, Japan

Received August 4, 2005

Metalladichalcogenolato cluster complexes [ $\{\text{CpCo}(\text{S}_2\text{C}_6\text{H}_4)\}_2\text{Mo}(\text{CO})_2$ ] ( $\text{Cp} = \eta^5\text{-C}_5\text{H}_5$ ) (**3**), [ $\{\text{CpCo}(\text{S}_2\text{C}_6\text{H}_4)\}_2\text{W}(\text{CO})_2$ ] (**4**), [ $\text{CpCo}(\text{S}_2\text{C}_6\text{H}_4)\text{Fe}(\text{CO})_3$ ] (**5**), [ $\text{CpCo}(\text{S}_2\text{C}_6\text{H}_4)\text{Ru}(\text{CO})_2(\text{P}^i\text{Bu}_3)$ ] (**6**), [ $\{\text{CpCo}(\text{Se}_2\text{C}_6\text{H}_4)\}_2\text{Mo}(\text{CO})_2$ ] (**7**), and [ $\{\text{CpCo}(\text{Se}_2\text{C}_6\text{H}_4)\}(\text{Se}_2\text{C}_6\text{H}_4)\text{W}(\text{CO})_2$ ] (**8**) were synthesized by the reaction of [ $\text{CpCo}(\text{E}_2\text{C}_6\text{H}_4)$ ] ( $\text{E} = \text{S}, \text{Se}$ ) with [ $\text{M}(\text{CO})_3(\text{py})_3$ ] ( $\text{M} = \text{Mo}, \text{W}$ ), [ $\text{Fe}(\text{CO})_5$ ], or [ $\text{Ru}(\text{CO})_3(\text{P}^i\text{Bu}_3)_2$ ], and their crystal structures and physical properties were investigated. In the series of trinuclear group 6 metal–Co complexes, **3**, **4**, and **7** have similar structures, but the W–Se complex, **8**, eliminates one cobalt atom and one cyclopentadienyl group from the sulfur analogue, **4**, and does not satisfy the 18-electron rule.  $^1\text{H}$  NMR observation suggested that the CoW dinuclear complex **8** was generated via a trinuclear  $\text{Co}_2\text{W}$  complex, with a structure comparable to **7**. The trinuclear cluster complexes, **3**, **4**, and **7**, undergo quasi-reversible two-step one-electron reduction, indicating the formation of mixed-valence complexes  $\text{Co}^{\text{III}}\text{M}^0\text{Co}^{\text{II}}$  ( $\text{M} = \text{Mo}, \text{W}$ ). The thermodynamic stability of the mixed-valence state increases in the order  $4 < 3 < 7$ . In the dinuclear group 8 metal–Co complexes, **5** and **6**, the  $\text{CpCo}(\text{S}_2\text{C}_6\text{H}_4)$  moiety and the metal carbonyl moiety act as a Lewis acid character and a base character, respectively, as determined by their spectrochemical and redox properties. Complex **5** undergoes reversible two-step one-electron reduction, and an electron paramagnetic resonance (EPR) study indicates the stepwise reduction process from  $\text{Co}^{\text{III}}\text{Fe}^0$  to form  $\text{Co}^{\text{III}}\text{Fe}^{-1}$  and  $\text{Co}^{\text{II}}\text{Fe}^{-1}$ .

### Introduction

Metalladichalcogenolenes of late transition metals exhibit unique electronic properties due to their quasi-aromaticity caused by strong  $d\pi\text{--}p\pi$  interaction, in which the metal center can be stabilized in unsaturated  $16e^-$  forms by the contribution of lone pair electrons in chalcogen (S, Se) atoms.<sup>1</sup> This electron deficiency of the metal center suggests the possibility of utilizing mononuclear metalladichalcogenolenes as building blocks of metal cluster complexes. In an exploration of this idea, we found a first example of a metal–metal bond formation of metalladithiolene complex; a reaction of [ $\text{CpCo}(\text{S}_2\text{C}_6\text{H}_4)$ ] (**1**) with [ $\text{Mo}(\text{CO})_3(\text{py})_3$ ]

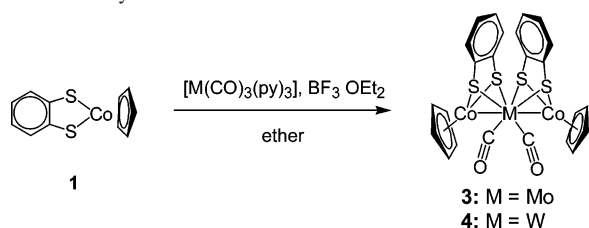
produced a trinuclear cluster complex [ $\{\text{CpCo}(\text{S}_2\text{C}_6\text{H}_4)\}_2\text{Mo}(\text{CO})_2$ ] (**3**) as reported in a communication.<sup>2</sup> This complex possesses a slightly bent Co–Mo–Co bond and extremely crooked cobaltadithiolene rings, indicating molecular orbital delocalization not only on the Co–Mo–Co bond but also on the metal–S bonds. This leads to thermal stability, the appearance of lower energy absorption bands in a VIS spectrum, and a reversible redox response.<sup>2</sup> We also synthesized the metalladiselenolene cluster complex, [ $\text{CpCo}(\text{Se}_2\text{C}_6\text{H}_4)_2$ ] (**2**),<sup>3</sup> which can be one of starting materials for this series of cluster complexes. It should be noted that Jin et al. have studied similar metal–metal bond formation reactions of carborane–dichalcogenolene complexes.<sup>4</sup> In this study, we investigated the reactions of **1** and **2** with groups

\* To whom correspondence should be addressed. E-mail: nishihara@chem.s.u-tokyo.ac.jp. Tel: +81 3 5841 4346. Fax: +81 5841 8063.

(1) (a) McCleverty, J. A. *Prog. Inorg. Chem.* **1969**, 2, 72. (b) Eisenberg, R. *Prog. Inorg. Chem.* **1970**, 12, 295. (c) Burns, R. P.; McAulliffe, C. A. *Adv. Inorg. Chem. Radiochem.* **1979**, 22, 303. (d) Fourmigue, M. *Coord. Chem. Rev.* **1998**, 178–180, 823. (e) Sugimori, A.; Akiyama, T.; Kajitani, M.; Sugiyama, T. *Bull. Chem. Soc. Jpn.* **1999**, 72, 879.

(2) Nihei, M.; Nankawa, T.; Kurihara, M.; Nishihara, H. *Angew. Chem., Int. Ed.* **1999**, 38, 1098.

(3) Habe, S.; Yamada, T.; Nankawa, T.; Mizutani, J.; Murata, M.; Nishihara, H. *Inorg. Chem.* **2003**, 42, 1952.

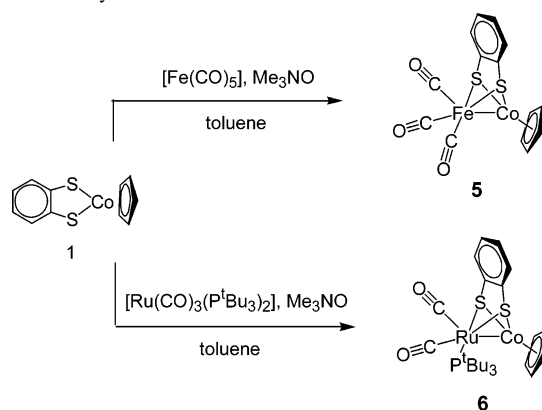
Scheme 1. Synthesis of **3** and **4**

**6** and **8** metal carbonyl complexes to determine the availability of this metal–metal bond formation of metalladichalcogenolenes and to compare the structures and properties of such cluster complexes and obtained novel trinuclear and dinuclear complexes bridged by the dichalcogenolato ligands with stoichiometry of  $\text{Co}_2\text{MoS}_4$  (**3**),  $\text{Co}_2\text{WS}_4$  (**4**),  $\text{CoFeS}_2$  (**5**),  $\text{RuCoS}_2$  (**6**),  $\text{Co}_2\text{MoSe}_4$  (**7**), and  $\text{CoWSe}_2$  (**8**). It is especially interesting that the  $\text{CoWSe}_2$  complex, **8**, does not satisfy the 18-electron rule. We herein describe the synthesis, molecular structure, and physical properties of these metalladichalcogenolene cluster complexes on the basis of the differences in the metal and chalcogen atoms as well as on the formation mechanism of **8**.

## Results and Discussion

**Synthesis and Characterization.** Reaction of  $[\text{CpCo}(\text{S}_2\text{C}_6\text{H}_4)]$  (**1**) with 0.5 equiv of  $[\text{M}(\text{CO})_3(\text{py})_3]$  ( $\text{M} = \text{Mo}$ ,  $\text{W}$ ) and 1.3–2.5 equiv of  $\text{BF}_3 \cdot \text{OEt}_2$  in diethyl ether at room temperature afforded two trinuclear dithiolene complexes,  $[\{\text{CpCo}(\text{S}_2\text{C}_6\text{H}_4)\}_2\text{Mo}(\text{CO})_2]$  (**3**) and  $[\{\text{CpCo}(\text{S}_2\text{C}_6\text{H}_4)\}_2\text{W}(\text{CO})_2]$  (**4**), in the form of dark brown crystals (Scheme 1). It is considered that the combination of  $[\text{M}(\text{CO})_3(\text{py})_3]$  and  $\text{BF}_3 \cdot \text{OEt}_2$  effectively generates a  $\text{M}(\text{CO})_3$  fragment,<sup>5</sup> which reacts with the cobaltadithiolene ring in **1**, forming two  $\text{M}–\text{Co}$  bonds. When the 12-electron  $\text{M}(\text{CO})_3$  fragment is generated, bonding with one molecule of **1** is not enough to satisfy the 18-electron rule at the  $\text{Mo}$  or  $\text{W}$  atom, and thus two molecules of **1** react with a  $\text{M}(\text{CO})_3$  fragment, followed by dissociation of one  $\text{CO}$  group to form the electronically satisfied trinuclear complex. The amount of  $\text{BF}_3 \cdot \text{OEt}_2$  adequate for the reaction was depending on the reaction conditions in the present cases (vide infra). The yields of **3** and **4** in the pure crystalline form were 34% and 11%, respectively, which is not due to occurrence of other reactions but due to decomposition in the purification process judging from the result of reaction monitoring by  $^1\text{H}$  NMR spectroscopy.

Treatment of **1** with 1.0 equiv of  $[\text{Fe}(\text{CO})_5]$  and 2.0 equiv of  $\text{Me}_3\text{NO}$  in toluene afforded a dinuclear complex,  $[\text{CpCo}(\text{S}_2\text{C}_6\text{H}_4)\text{Fe}(\text{CO})_3]$  (**5**), in the form of green crystals in a moderate yield (Scheme 2). In this case, a 16-electron  $\text{Fe}(\text{CO})_4$  fragment was initially generated from  $[\text{Fe}(\text{CO})_5]$  by treatment with  $\text{Me}_3\text{NO}$ ,<sup>6</sup> and the cobaltadithiolene ring in **1** was subjected to nucleophilic attack by the fragment ac-

Scheme 2. Synthesis of **5** and **6**

companied by the formation of a  $\text{Co}–\text{Fe}$  bond. Assuming that the cobaltadithiolene ring can provide 4 electrons to the  $\text{Fe}(\text{CO})_4$  moiety, the iron atom satisfies the 18-electron rule through the formation of **5** with the elimination of one  $\text{CO}$ . This suggests that the number of cobaltadithiolene molecules bound to the metal carbonyl fragment can be adjusted by changing the number of electrons on the fragment. A similar reaction using  $[\text{Ru}(\text{CO})_3(\text{P}^t\text{Bu}_3)_2]$ <sup>7</sup> instead of  $[\text{Fe}(\text{CO})_5]$  gave a yellow solid,  $[\text{CpCo}(\text{S}_2\text{C}_6\text{H}_4)\text{Ru}(\text{CO})_2(\text{P}^t\text{Bu}_3)]$  (**6**).

A trinuclear diselenolene complex,  $[\{\text{CpCo}(\text{Se}_2\text{C}_6\text{H}_4)\}_2\text{Mo}(\text{CO})_2]$  (**7**), was obtained as dark brown crystals by the reaction of a cobaltadiselenolene compound **2**, which is in equilibrium between monomeric and dimeric forms in solution,<sup>3</sup> with 1.0 equiv of  $[\text{Mo}(\text{CO})_3(\text{py})_3]$  and 3.0 equiv of  $\text{BF}_3 \cdot \text{OEt}_2$  in diethyl ether at room temperature in 28% yield. We found that a Lewis acid  $\text{BF}_3 \cdot \text{OEt}_2$  is not required in the preparation of **7** in dichloromethane having a low donor number, resulting in higher product yield (95%) (Scheme 3).

Surprisingly, a dinuclear diselenolene complex  $[\{\text{CpCo}(\text{Se}_2\text{C}_6\text{H}_4)(\text{Se}_2\text{C}_6\text{H}_4)\text{W}(\text{CO})_2]$  (**8**) was obtained by the reaction of **2** with 1.0 equiv of  $[\text{W}(\text{CO})_3(\text{py})_3]$  in the presence of more than 10 equiv of  $\text{BF}_3 \cdot \text{OEt}_2$  in diethyl ether under reflux (Scheme 3). This reaction did not proceed without the additive or without heating in diethyl ether. On the other hand, the reaction in toluene with 5 equiv of  $\text{BF}_3 \cdot \text{OEt}_2$  proceeded at room temperature, indicating that the reaction processes were highly depending on the polarity of solvent, the differences in stability of  $[\text{M}(\text{CO})_3(\text{py})_3]$  complexes, and the coordination ability of  $\text{S}$  or  $\text{Se}$  in chalcogenolenes. In the structure of **8**, the  $\text{Co}$  and  $\text{Cp}$  were removed from a  $\text{Co}_2\text{W}$  trinuclear complex analogous to the dithiolene complex, **4** (vide infra).

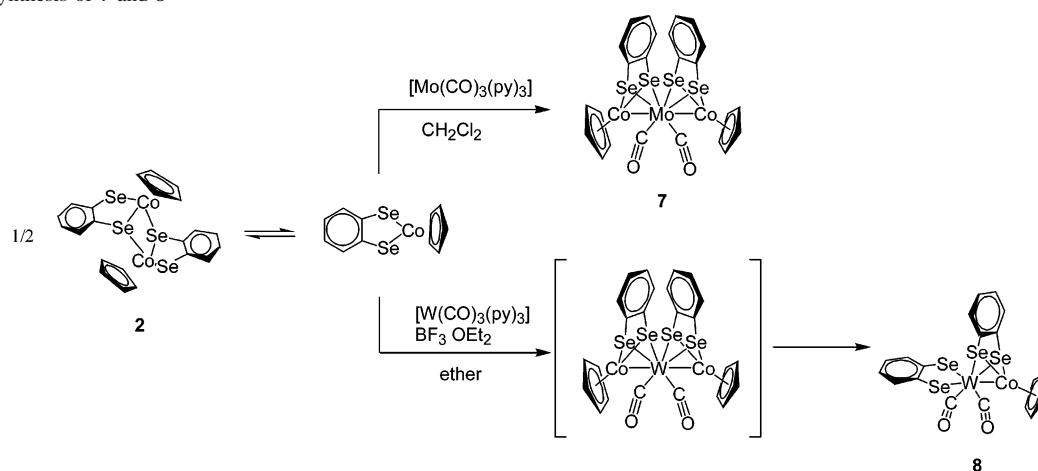
**Molecular Structure.** The molecular structures of **3**–**5**, **7**, and **8** were determined by single-crystal X-ray crystallography. Crystallographic data are summarized in Table 1. All three trinuclear complexes, **3**, **4**, and **7**, were found to have similar structures, in which the central  $\text{Mo}$  or  $\text{W}$  atom is eight-coordinate with a square-antiprismatic geometry. An ORTEP drawing of **7** is displayed in Figure 1, and a comparison of selected bond lengths and angles between the three complexes is shown in Table 2. The  $\text{Co}–\text{S}$  bond

(4) (a) Wang, J.-Q.; Weng, L.-H.; Jin, G.-X. *J. Organomet. Chem.* **2005**, *690*, 249. (b) Jin, G.-X.; Wang, J.-Q.; Zhang, C.; Weng, L.-H.; Herberhold, M. *Angew. Chem., Int. Ed.* **2005**, *44*, 259.

(5) Nesmeyanov, A. N.; Krivykh, V. V.; Kaganovich, V. S.; Rybinskaya, M. I. *J. Organomet. Chem.* **1975**, *102*, 185.

(6) Shvo, Y.; Hazum, E. *J. Chem. Soc., Chem. Commun.* **1975**, 829.

(7) Schumann, H.; Opitz, J. *J. Organomet. Chem.* **1979**, *166*, 233.

Scheme 3. Synthesis of **7** and **8**Table 1. Crystallographic Data for **3**–**5**, **7**, and **8**

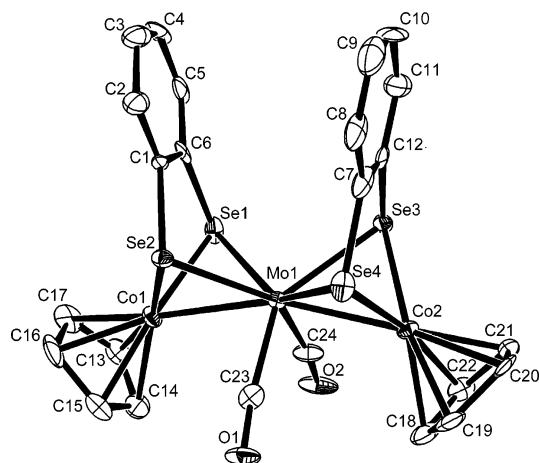
param	<b>3</b>	<b>4</b>	<b>5</b>	<b>7</b>	<b>8</b>
empirical formula	$\text{C}_{24}\text{H}_{18}\text{Co}_2\text{MoO}_2\text{S}_4$	$\text{C}_{24}\text{H}_{18}\text{Co}_2\text{O}_2\text{S}_4\text{W}$	$\text{C}_{14}\text{H}_9\text{CoFeO}_3\text{S}_2$	$\text{C}_{24}\text{H}_{18}\text{Co}_2\text{MoO}_2\text{Se}_4$	$\text{C}_{19}\text{H}_{13}\text{CoO}_2\text{Se}_4\text{W}$
fw	680.45	768.36	404.12	868.05	831.91
cryst system	triclinic	triclinic	monoclinic	monoclinic	triclinic
<i>a</i> (Å)	12.040(3)	11.672(2)	10.922(2)	6.6624(7)	8.079(5)
<i>b</i> (Å)	15.858(4)	16.107(4)	12.611(1)	23.145(2)	10.432(6)
<i>c</i> (Å)	6.587(2)	6.505(1)	10.960(2)	16.511(2)	13.196(8)
$\alpha$ (deg)	101.89(2)	96.27(2)			66.93(2)
$\beta$ (deg)	98.86(2)	96.18(1)	90.28(1)	102.433(6)	81.35(3)
$\gamma$ (deg)	92.78(2)	84.12(2)			77.75(3)
space group	$P\bar{1}$ (No. 2)	$P\bar{1}$ (No. 2)	$P2_1/a$ (No. 14)	$P2_1$ (No. 4)	$P\bar{1}$ (No. 2)
<i>V</i> (Å <sup>3</sup> )	1211.8(6)	1203.5(4)	1509.5(4)	2486.3(5)	997.1(10)
<i>Z</i> value	2	2	4	4	2
$\rho_{\text{calcd}}$ (g/cm <sup>3</sup> )	1.865	2.12	1.778	2.319	2.771
$\mu$ (cm <sup>-1</sup> )	22.3	65.04	23.4	76.93	139.1
<i>T</i> (K)	296	293	296	120	120
no. of observns	4707	4217	2617	5456	4510
residuals: <i>R</i> ; <i>wR</i>	0.041, 0.040	0.038, 0.044	0.051, 0.041	0.033, 0.053	0.091, 0.245
GOF		1.330	6.86	1.470	1.124

lengths of **3** and **4** are 2.214(2) Å and 2.217(2) Å, respectively, that are ca. 0.10 Å longer than that of a free cobaltadithiolene ring.<sup>8</sup> The Co–Mo bond length in **3** is 2.626(1) Å, which is within the range of a regular Co–Mo single bond length.<sup>9</sup> In the structure of **4**, the Co–W (2.581(1) Å) and S–W (2.481(2) Å) bond lengths are shorter than those of the Co–Mo (2.626(1) Å) and S–Mo (2.497(1) Å) bonds in **3**, respectively. On the other hand,

the C–W bond length (2.014(9) Å) is longer than that of the C–Mo (1.987(6) Å) bond in **3**. It is considered that the  $\sigma$ -donation from W to Co is stronger than that from Mo to Co, while the  $\pi$ -back-donation from W to CO is weaker than that from Mo to CO.

In the structure of a diselenolato complex, **7**, the average Co–Mo bond length is 2.637(2) Å, which is also within the usual range for Co–Mo single bonds<sup>9</sup> and a little longer than that of the S analogue **3** (2.626(1) Å) (see Table 2). The differences in bond lengths of E–Co and E–Mo (E = S, Se) between these two complexes are smaller than the difference between the covalent radii of Se and S, suggesting that the Se–Co and Se–Mo bonds are stronger than the S–Co and S–Mo bonds, respectively. The Se atom, which has a higher electron density than the S atom and an energy level closer to those of the transition metals, is easier to use for the formation of a bridge structure between Co and Mo.

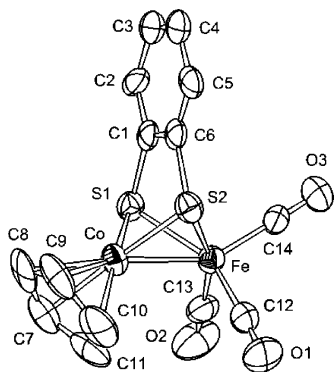
An ORTEP drawing of the CoFe dinuclear complex, **5**, is displayed in Figure 2. The distance between the cobalt and the iron atoms is 2.420(1) Å, indicating a single metal–metal bond nature (see Table 3). Each metal atom is

Figure 1. ORTEP drawing of **7** with 50% probability ellipsoids and H atoms omitted.(8) Miller, E. J.; Brill, T. B.; Rheingold, A. L.; Fultz, W. C. *J. Am. Chem. Soc.* **1983**, *105*, 7580.(9) Curtis, M. D.; Druker, S. H.; Goossen, L.; Kampf, J. W. *Organometallics* **1997**, *16*, 231.

**Table 2.** Selected Bond Lengths (Å) and Angles (deg) of **3**, **4**, and **7**

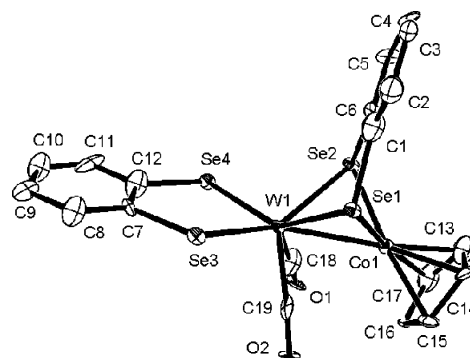
bond	<b>3</b>	<b>4</b>	<b>7</b>
	(M = Mo, E = S)	(M = W, E = S)	(M = Mo, E = Se) <sup>a</sup>
M1–Co1	2.6182(8)	2.581(1)	2.633(1)
M1–Co2	2.6327(9)	2.581(1)	2.641(1)
M1–E1	2.478(1)	2.477(2)	2.580(1)
M1–E2	2.520(1)	2.484(2)	2.611(2)
M1–E3	2.514(1)	2.479(2)	2.626(1)
M1–E4	2.477(1)	2.484(2)	2.606(1)
M1–C23	1.983(6)	2.032(7)	1.963(8)
M1–C24	1.990(6)	1.996(9)	1.982(8)
Co1–E1	2.199(2)	2.221(2)	2.317(1)
Co1–E2	2.237(2)	2.216(2)	2.349(2)
Co2–E3	2.227(2)	2.216(2)	2.345(1)
Co2–E4	2.191(2)	2.216(3)	2.306(2)
C23–O1	1.156(6)	1.11(1)	1.14(1)
C24–O2	1.150(6)	1.14(1)	1.15(1)
E1–C1	1.787(5)	1.779(8)	1.923(7)
E2–C6	1.792(5)	1.782(7)	1.932(8)
E3–C7	1.778(5)	1.78(1)	1.940(8)
E4–C12	1.785(5)	1.783(7)	1.936(8)
Co1–C13	2.051(6)	2.06(1)	2.049(8)
Co1–C14	2.081(6)	2.06(1)	2.052(8)
Co1–C15	2.064(6)	2.052(9)	2.073(9)
Co1–C16	2.079(6)	2.06(1)	2.06(1)
Co1–C17	2.056(6)	2.07(1)	2.050(9)
Co2–C18	2.075(6)	2.04(1)	2.064(8)
Co2–C19	2.067(6)	2.06(1)	2.054(8)
Co2–C20	2.059(6)	2.09(1)	2.058(8)
Co2–C21	2.088(7)	2.09(1)	2.062(9)
Co2–C22	2.049(7)	2.04(1)	2.045(8)
M1–C23–O1	171.8(5)	173.1(8)	170.3(7)
M1–C24–O2	171.7(5)	174.1(6)	169.7(8)
Co1–M1–Co2	165.03(3)	161.99(4)	160.53(5)

<sup>a</sup> The selected bond lengths and angles of **7** are the average values of two crystallographically independent molecules.

**Figure 2.** ORTEP drawing of **5** with 50% probability ellipsoids and H atoms omitted.**Table 3.** Selected Bond Lengths (Å) and Angles (deg) of **5**

Fe1–Co1	2.420(1)	C12–O1	1.127(6)
Fe1–S1	2.287(2)	C13–O2	1.137(7)
Fe1–S2	2.287(2)	C14–O3	1.129(6)
Co1–S1	2.207(2)	Co1–Fe1–S1	55.84(4)
Co1–S2	2.193(2)	Co1–Fe1–S2	55.43(5)
Fe1–C12	1.794(6)	Fe1–C12–O1	176.5(5)
Fe1–C13	1.771(6)	Fe1–C13–O2	178.5(6)
Fe1–C14	1.793(6)	Fe1–C14–O3	179.0(6)

coordinated by two sulfur atoms of a benzenedithiolato ligand; presumably, one CoCp moiety and one Fe(CO)<sub>3</sub> moiety are connected by a metal–metal bond supported by a benzenedithiolato ligand. Through the formation of a benzenedithiolato bridge, the planarity of the CoS<sub>2</sub>C<sub>2</sub> ring is lost, which occurs also in the previously described Co<sub>2</sub>Mo complex **3**.

**Figure 3.** ORTEP drawing of **8** with 50% probability ellipsoids and H atoms omitted.**Table 4.** Selected Bond Lengths (Å) and Angles (deg) of **8**

W1–Co1	2.626(3)	Co1–Se1	2.350(3)
W1–Se1	2.593(2)	Co1–Se2	2.347(3)
W1–Se2	2.587(2)	C18–O1	1.13(2)
W1–Se3	2.496(2)	C19–O2	1.13(2)
W1–Se4	2.496(2)	W1–C18–O1	175(2)
W1–C18	2.01(2)	W1–C19–O2	175(2)
W1–C19	2.01(2)		

An ORTEP drawing of **8** is displayed in Figure 3. The W center is seven-coordinate with one less Co atom and one less Cp group, being distinct from **7**. The cobaltadisenolene ring is nonplanar due to the coordination of the Se atoms to W, while the tungstenadisenolene ring is planar. The number of total valence electrons around the CoW core is 32; the two Se atoms at the bridging diselenolato ligand each contribute three electrons. The complex is electronically sufficient if there is a Co–W double bond, but the W–Co bond length is 2.626(3) Å (Table 4) indicating a single bond character. This implies that the complex is electron deficient or coordinatively unsaturated (a further discussion on the stability of **8** is given below). It is possible that **8** receives a small molecule, which activates it at vacant coordination positions by virtue of the electron density donated by the late transition metal atom Co, which undergoes a reversible redox reaction. Bis(dithiolene)tungsten complexes are studied from the standpoint of the model complexes of the active sites of molybdoenzymes in the DMSO reductase family.<sup>10</sup> To our knowledge, **8** is the first complex to include such a metal–metal bond and may provide some important new information regarding the biomolecule. Its C–O bond length is shorter than that of **5**, indicating that the back-donation from W to CO is weaker than it is in **5**.

**Spectroscopic Properties.** The spectroscopic data for characteristic IR, VIS, and <sup>1</sup>H NMR bands and redox properties of cluster complexes **3–7** are summarized in Table 5 with **1** and **2** as references. The IR spectra of the trinuclear complexes, **3**, **4**, and **7**, showed that each complex had two ν(CO) bands, which is consistent with the C<sub>2</sub> symmetry at the Mo or W center. The C–O bond strength in the diselenolene compound, **7**, is weaker than that in the dithiolene compound, **3**, by ca. 20 cm<sup>−1</sup>, indicating that the electron density of the carbonyl groups is increased by the back-donation from the Mo atom, the density of which is

(10) Sung, K.-M.; Holm, R. H. *J. Am. Chem. Soc.* **2002**, *124*, 4312.

**Table 5.** Spectroscopic and Electrochemical Properties of Compounds **1–8**

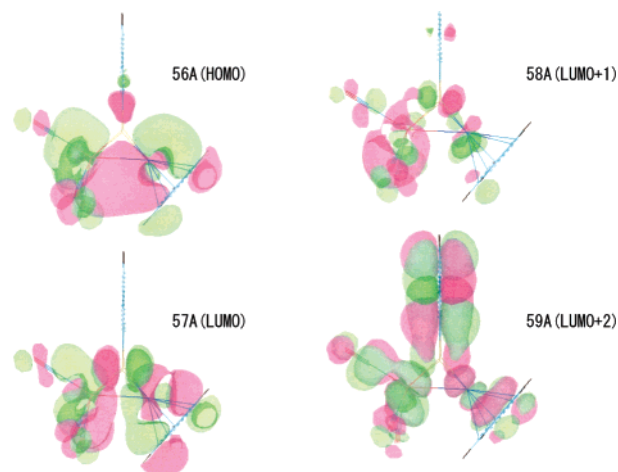
param	<b>1</b>	<b>2</b>	<b>3</b>	<b>4</b>	<b>5</b>	<b>6</b>	<b>7</b>	<b>8</b>
$\nu_{\text{CO}}/\text{cm}^{-1}$ (KBr disk)			1923 1860	1927 1856	2038 1995 1956	1978 1928	1901 1839	1977 1921
$^1\text{H NMR: } \delta/\text{ppm}$ (in $\text{CD}_3\text{Cl}$ )								
Cp	5.49	5.69 <sup>b</sup>	5.15	4.72	4.62	4.96	5.09	5.17
Ph	7.31	7.24 <sup>b</sup>	6.34	6.17	6.04	6.20	6.48	6.86, 7.29
	8.11	8.13	6.79	6.97	6.81	7.04	6.95	7.50, 8.38
$\lambda_{\text{max}}/\text{nm}$ (in toluene)	576	581	476	446	606	586	478	385
$\epsilon_{\text{max}}/\text{M}^{-1} \text{cm}^{-1}$	9730	3200	7060	14 700	977	971	8970	9500
$E_{\text{red}}^{\text{oc}}/\text{V}$ vs $\text{Fc}^+/\text{Fc}$	-1.18 (r)	-0.78 (r)	-1.41 (r)	-1.49 (r)	-1.48 (r)	-1.72 (ir)	-1.13 (r)	-1.37 (r) <sup>a</sup>
$E_{\text{red}}^{\text{oc}}/\text{V}$ vs $\text{Fc}^+/\text{Fc}^+$			-1.74 (r)	-1.73 (r)	-1.78 (r)		-1.55 (r)	
$\Delta E^{\text{oc}}/\text{V}$			0.33	0.24	0.30		0.42	

<sup>a</sup> In  $\text{CH}_2\text{Cl}_2$ ; others are in MeCN. <sup>b</sup> In  $\text{DMSO}-d_6$ .

heightened by the exchange of S with Se. The CoW dinuclear compound, **8**, also exhibits two  $\nu(\text{CO})$  bands, one at 1977 and the other at 1921  $\text{cm}^{-1}$ , but the wavenumbers are significantly higher than those of the trinuclear complexes. The weaker back-donation in **8** is due to the decrease in the electron density of the W atom in the presence of the additional benzenediselenolene ring which retains planarity. These IR spectroscopic observations substantiated the results of the single-crystal X-ray crystallography as noted above. The CoFe and RuCo dinuclear complexes, **5** and **6**, show three and two  $\nu(\text{CO})$  bands, respectively, which are located at higher wavenumbers compared with the Mo and W complexes. This might suggest that the electron donation of Fe or Ru to Co is stronger than that of Mo or W to Co.

$^1\text{H NMR}$  spectroscopy indicated that all the compounds obtained are diamagnetic.  $^1\text{H NMR}$  signals of the Cp ring and the phenylene moiety in the cluster complexes, **3–8**, are shifted to higher fields than is the case in the monomeric complexes, **1** and **2**, as given in Table 5. This can be ascribed also to the electron donation effect of Mo, W, or Fe to Co; this effect increases the electron density to Cp and the benzenedichalcogenato ligand around the Co center. Larger shifts of both signals in **3**, **4**, **7**, and **8** than in **5** and **6** might be caused by the stronger electron donation of Fe and Ru compared with Mo and W, which has been suggested in the  $\nu(\text{CO})$  frequency as noted above. It should be noted that the  $^1\text{H NMR}$  signal of the Cp ring in **8** was changed from  $\delta$  5.17 ppm in chloroform-*d* to 4.46 ppm in benzene-*d*<sub>6</sub> (see Figure 8), indicating an existence of the significant solvent effect.

A characteristic feature of cobaltadithiolane is a strong absorption due to the ligand-to-metal charge-transfer (LMCT) transition in the visible region.<sup>11</sup> This is intimately related to the aromatic nature of the metalladithiolene ring. In all the cluster complexes, the planarity of the cobaltadithiolene ring is lost, indicating a decrease in the aromatic nature. This may influence the visible absorption spectrum; indeed, the band is shifted to higher energy in complexes **3** (476 nm), **4** (446 nm), **7** (478 nm), and **8** (385 nm) compared with the monomeric complexes **1** (576 nm) and **2** (581 nm). In the

**Figure 4.** 56A (HOMO), 57A (LUMO), 58A (LUMO + 1), and 59A (LUMO + 2) orbitals of **5** obtained by ZINDO calculation.**Table 6.** Contribution Ratios of Co, Fe, and S Atoms to Molecular Orbitals

atom	56A (HOMO)	57A (LUMO)	58A	59A
Co	0.345	0.404	0.371	0.103
Fe	0.412	0.240	0.445	0.129
S	0.013	0.007	0.005	0.028

dinuclear complexes, **5** and **6**, the lowest energy absorption appears at 606 and 586 nm, respectively, indicating lower energy compared with **1**. We postulate that this band is not the LMCT band of the cobaltadithiolene moiety, since planarity is lost, but rather the transition from the  $\text{Co}-\text{M}'$  ( $\text{M}' = \text{Fe}, \text{Ru}$ )  $\sigma$ -bonding orbital to the  $\text{Co}-\text{M}' \sigma^*$ -orbital, since the energy levels of the Fe and Co d-orbitals are located close to one another, according to a semiempirical molecular orbital calculation using the ZINDO method<sup>12</sup> (see LUMO and HOMO in Figure 4 and Table 6).

**Redox Properties.** Cyclic voltammograms (CV's) of **7** at 0.1  $\text{V s}^{-1}$  in  $\text{Bu}_4\text{NClO}_4\text{-MeCN}$  are shown in Figure 5. The first cyclic scan between -0.4 and -1.8 V vs ferrocenium/ferrocene ( $\text{Fc}^+/\text{Fc}$ ) showed two couples of reduction and reoxidation waves at  $E^{\text{oc}} = -1.13$  and -1.55 V and an oxidation wave at  $E_{\text{p,a}} = -0.78$  V. A reduction wave corresponding to this oxidation wave was observed at  $E_{\text{p,c}} = -0.96$  V in the second cyclic scan. This additional redox

(11) (a) Baker-Hwkes, M. J.; Billif, E.; Gray, H. B. *J. Am. Chem. Soc.* **1966**, *88*, 4870. (b) Shupack, S. I.; Billif, E.; Clark, R. J. H.; Williams, R.; Gray, H. B. *J. Am. Chem. Soc.* **1964**, *86*, 4594. (c) Schrauzer, G. N.; Mayweg, V. P. *J. Am. Chem. Soc.* **1965**, *87*, 3585.

(12) Anderson, W. P.; Edwar, W. D.; Zerner, M. C. *Inorg. Chem.* **1986**, *25*, 2728.

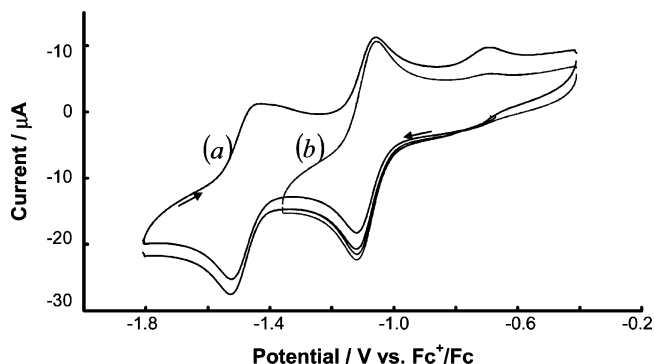


**Figure 5.** Cyclic voltammograms of **7** (−0.4 to −1.4 V (a) and −0.4 to −1.8 V (b)) at a glassy carbon disk at a scan rate of 0.1 V s<sup>−1</sup> in 0.1 M Bu<sub>4</sub>NClO<sub>4</sub>–MeCN.

couple was determined to be 2<sup>0</sup>/2<sup>−</sup> by the consistency of  $E^0$ .<sup>2</sup> It should be noted that the oxidation wave at −0.78 V did not appear when the potential scan was in a range between −0.4 and −1.4 V causing only the first-step reduction of **7**. These results indicate that the reduction of **7** gives monoanion and dianion successively, and then the dianion decomposes to give 2 × 2<sup>−</sup> and a “Mo(CO)<sub>2</sub>” fragment, whose fate has not been determined. Thus the redox process of **7** can be expressed as the following EEC mechanism:



The rate constant of the decomposition reaction of 7<sup>2−</sup>,  $k$ , was estimated by a computer simulation of CV to be 0.04 s<sup>−1</sup>.

Cyclic voltammetry of each of the other trinuclear complexes, **3** and **4**, also showed two quasi-reversible 1e<sup>−</sup> reduction waves with the appearance of a small oxidation peak after the 2e<sup>−</sup> reduction, at a scan rate of 0.1 V s<sup>−1</sup> (see Table 5). The peak due to the generation of **1** or **2** depends on both metal and chalcogen atoms, and the decomposition rate constants for **3** and **4** are 0.19 and 0.02 s<sup>−1</sup>, respectively, indicating an order of stability of 3<sup>2−</sup> ≪ 7<sup>2−</sup> < 4<sup>2−</sup>; the Se bridge stabilizes the complex much more than does the S bridge, and the W–Co bond is stronger than the Mo–Co bond in the 2<sup>−</sup> valence state. In comparing the redox potentials among the three complexes, it is reasonable to assume that the two Co centers, but not the Mo or W atoms, undergo reduction. All the cluster complexes synthesized in this study are diamagnetic, show a visible band characteristic of the original mononuclear metalladithiolene in the absorption spectra, and are reduced at a potential similar to that of the original metalladithiolene, indicating that the oxidation state of the metal in the metalladithiolene does not change by forming metal–metal bonds. Therefore, the formal oxidation states in the neutral form can be written as Co<sup>III</sup>–Mo<sup>0</sup>Co<sup>III</sup> (**3**), Co<sup>III</sup>W<sup>0</sup>Co<sup>III</sup> (**4**), Co<sup>III</sup>Fe<sup>0</sup> (**5**), Ru<sup>0</sup>Co<sup>III</sup> (**6**), Co<sup>III</sup>–Mo<sup>0</sup>Co<sup>III</sup> (**7**), and Co<sup>III</sup>W<sup>0</sup> (**8**). This implies that the valency balance of monoanions of **3**, **4**, and **7** can be expressed as

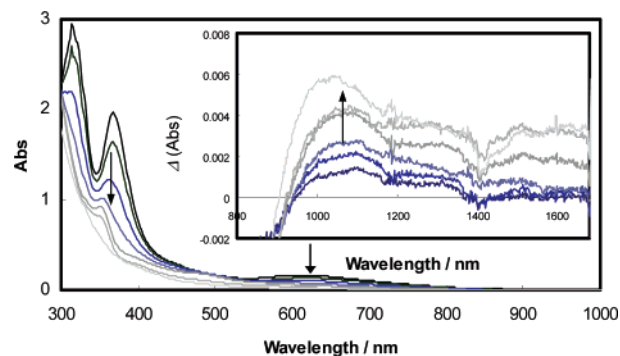


**Figure 6.** Changes in UV–vis spectra of **5** by stepwise reduction with Na in 2-MeTHF. Inset: Differences in the spectra of **5** in the NIR region caused by the reduction from the original spectrum of **5**.

Co<sup>III</sup>M<sup>0</sup>Co<sup>II</sup> (M = Mo, W), suggesting that the Mo or W bridge assists the electronic interaction between Co sites to form a thermodynamically favorable mixed-valence state.<sup>13,14</sup> This is supported by the electronic spectrum of **3**<sup>−</sup> generated by the reduction of **3** with Na in THF, where a broad band attributable to an intervalence transfer<sup>13,14</sup> appears at 1160 nm ( $\epsilon = 60 \text{ M}^{-1} \text{ cm}^{-1}$ ). Judging from the  $\Delta E^0$  values, the thermodynamic stability of the mixed-valence state increases in the order **4** < **3** < **7**. It is postulated that the unoccupied d-orbital of W, which is at a higher level than that of Mo, assists less effectively in the electronic communication between the two Co sites and that one introduced electron is more liable to delocalize via the Se bridge than via the S bridge because Se is softer and easier to polarize than S.

A cyclic voltammogram of the CoFe complex **5** in THF exhibited two 1e<sup>−</sup> reversible reduction waves at  $E^0 = -1.48$  and  $-1.78 \text{ V vs Fc}^+/\text{Fc}$ . The high stability of 5<sup>2−</sup> is in contrast to the Co<sub>2</sub>Mo complex **3**, which is subject to dissociation into **1** by two-electron reduction.<sup>2</sup> Electronic structures of the reduced forms of **5** were examined on the basis of the electronic and EPR spectra. In the UV–vis–NIR spectra in Figure 6, the characteristic band of **5** at 606 nm decreased continuously by one- and two-electron reductions with Na in 2-MeTHF. Concurrently, a weak broad band ( $\epsilon_{\text{max}} = 12 \text{ M}^{-1} \text{ cm}^{-1}$ ) appeared in the NIR region at 1100 nm by the first reduction and, in response to the second reduction, shifted slightly to a higher energy at 1030 nm and increased in intensity ( $\epsilon_{\text{max}} = 34 \text{ M}^{-1} \text{ cm}^{-1}$ ). The appearance of the low-energy band suggests that electronic isomers, such as valence tautomers, with similar ground-state energies exist in both reduced forms.

It is interesting to see whether the iron or cobalt site is reduced first. We measured the EPR spectra of 5<sup>−</sup> and 5<sup>2−</sup> generated by stepwise reduction with Na in THF while monitoring their UV–vis–NIR spectra carefully at 7 K, and the results are displayed in Figure 7. The spectrum in the monoanionic state indicates anisotropic signals at  $g_x = 2.004$ ,  $g_y = 2.038$ , and  $g_z = 2.064$  without hyperfine octet splitting

(13) Hush, N. S. *Prog. Inorg. Chem.* **1967**, *8*, 391–444.

(14) (a) Okuno, M.; Aramaki, K.; Nakajima, S.; Watanabe, T.; Nishihara, H. *Chem. Lett.* **1995**, 585. (b) Okuno, M.; Aramaki, K.; Nishihara, H. *J. Electroanal. Chem.* **1997**, *438*, 79. (c) Nishihara, H.; Okuno, M.; Akimoto, N.; Kogawa, N.; Aramaki, K. *J. Chem. Soc., Dalton Trans.* **1998**, 2651.

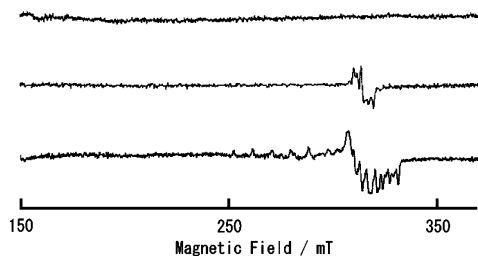


**Figure 7.** EPR spectra of  $5^-$  and  $5^{2-}$  generated by stepwise reduction with Na in THF at 7 K.

due to the Co nucleus with  $I = 7/2$ , indicating that the first electron introduced is located not at the cobalt center but at the iron center;<sup>15</sup> that is, the valence state is changed formally from  $\text{Fe}^0\text{Co}^{\text{III}}$  to  $\text{Fe}^{-1}\text{Co}^{\text{III}}$ . The LUMO of **5**, calculated using the ZINDO method on the basis of the structure obtained by X-ray analysis, indicates that the orbital is delocalized on the Co–Fe bond but that Co d-orbitals contribute more than Fe d-orbitals (see Figure 4 and Table 6). This is not fully consistent with the EPR result described above, and a more restrictive calculation of the anionic form is necessary for further discussion. The second reduction to form  $5^{2-}$  gave a spectrum with hyperfine splitting<sup>14c</sup> with signals of the Fe center. It is not easy to separate the signals of Co and Fe or to get more information on the magnetic properties of  $5^{2-}$  at present, since  $5^{2-}$  is highly sensitive to oxygen. However, we can postulate from the EPR study that  $5^{2-}$  is in the valence state of  $\text{Fe}^{-1}\text{Co}^{\text{II}}$  and that the spins exist at both metals and are not antiferromagnetically coupled at 7 K.

The CoRu complex **6**, in contrast, showed only a broad irreversible reduction wave at  $E_{p,c} = -1.72$  V vs ferrocene/ferrocenium, suggesting that the skeleton of **6** is easily decomposed upon reduction.

**Pathway of the Formation of 8.** The molecular structure of **8** indicates that one cobaltadiselenolene ring is broken and that the diselenolene ligand that was coordinating to the Co atom in **2** migrates to the W atom in **8** in the formation process. There are some examples of ligand transfer in the dithiolene chemistry,<sup>16</sup> but there has been no example of a diselenolato ligand. To examine the reaction mechanism, we synthesized **8** in an NMR tube and measured spectral change with increasing temperature and reaction time, and those time course changes are shown in Figure 8. At first, **2** and  $[\text{W}(\text{CO})_3(\text{py})_3]$  were dissolved in benzene- $d_6$ , to which  $\text{BF}_3 \cdot \text{OEt}_2$  was then added. In the course of the reaction at room temperature, an intermediate with smaller  $\delta$  values for benzene and Cp ring protons compared with those of **8** gradually formed (dotted arrows). Then **8** (solid arrows) was generated with increasing temperature, accompanied by a reduction of the intermediate. Our attempt to isolate the intermediate in the reaction of **2** with  $[\text{W}(\text{CO})_3(\text{py})_3]$  in toluene (vide supra) gave an thermally unstable complex of which spectral data can be assigned to a trinuclear  $\text{Co}_2\text{W}$  complex with a structure comparable to **7** in addition to **8**

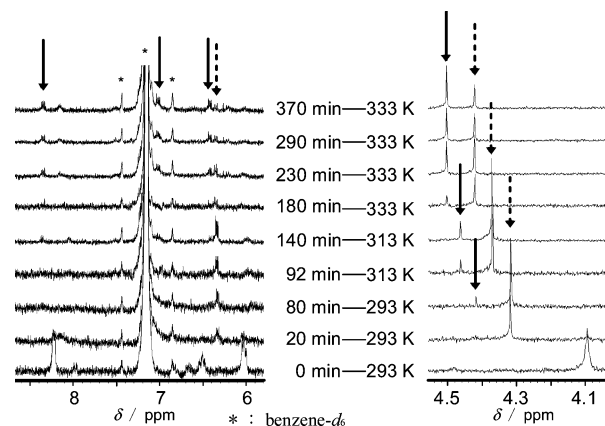


**Figure 8.**  $^1\text{H}$  NMR spectral change during the pursuit of the synthetic process on **8** in benzene- $d_6$ . The signals of the intermediate and **8** are denoted by dotted and solid arrows, respectively. Reaction time and temperature are listed in each chart.

(see Experimental Section). These results strongly suggest that the trinuclear  $\text{Co}_2\text{W}$  complex was initially formed, followed by a decrease with increasing temperature in the amount and generation of dinuclear complex **8** (see Scheme 3).

It is intriguing that the electron-deficient CoW dinuclear complex, **8** (vide supra), has higher thermodynamic stability than the  $\text{Co}_2\text{W}$  trinuclear complex which is electronically satisfied. The analogous  $\text{Co}_2\text{W}$  dithiolato and  $\text{Co}_2\text{Mo}$  diselenolato trinuclear complexes, **4** and **7**, respectively, are thermally stable and do not give dinuclear complexes. One possible rationale of this difference would take into account the HSAB principle, that the combination of soft W and soft Se atoms eliminates one of the hard Co atoms, but other combinations with less-soft Mo and/or less-soft S atoms have an affinity for two Co atoms. Elimination of the CoCp moiety from the  $\text{Co}_2\text{W}$  trinuclear complex affords a planar tungstenadiselenolene ring with high aromaticity, and thus the electron-deficient dinuclear complex can be stable. To address these issues, further investigations of the synthesis of cluster complexes with other metal–metal–chalcogen combinations are currently under way in our laboratory.<sup>17</sup>

## Conclusion

A series of heterometal cluster complexes were synthesized by a metal–metal bond formation reaction of the cobaltadichalcogenolene (S, Se) with the group 6 (Mo, W) and 8 (Fe, Ru) metal carbonyls. Group 6 metal (M)–Co complexes, **3**, **4**, and **7**, have Co–M–Co linear trinuclear structures with two bridging benzenedicalcogenolato ligands, whereas the W–cobaltadiselenolene complex, **8**, has a W–Co dinuclear structure, formed by elimination of one cobalt atom and one cyclopentadienyl group from the trinuclear complex. Group 8 metal (M′)–Co complexes, **5** and **6**, have Co–M′ dinuclear structures with a bridging benzenedicalcogenolato ligand. Electrochemistry of the cluster complexes showed quasi-reversible reductions in most of the cases. Two-step one-electron reduction takes place in the trinuclear cluster

(15) Peake, B. M.; Symons, M. C. R.; Wyatt, J. L. *J. Chem. Soc., Dalton Trans.* **1983**, 1171.

(16) (a) Seidel, W. W.; Hahn, F. E. *J. Chem. Soc., Dalton Trans.* **1999**, 2237. (b) Goddard, C. A.; Holm, R. H. *Inorg. Chem.* **1999**, *38*, 5389.

(17) Nakagawa, N.; Yamada, T.; Murata, M.; Sugimoto, M.; Nishihara, H. *Inorg. Chem.* **2006**, *45*, 14.

complexes, **3**, **4**, and **7**, forming  $\text{Co}^{\text{III}}\text{M}^0\text{Co}^{\text{II}}$  via a mixed-valence state  $\text{Co}^{\text{III}}\text{M}^0\text{Co}^{\text{II}}$ . A dinuclear complex **5** also undergoes two-step one-electron reduction, where the oxidation state changes from  $\text{Co}^{\text{III}}\text{Fe}^0$  to form  $\text{Co}^{\text{III}}\text{Fe}^{-1}$  and then  $\text{Co}^{\text{II}}\text{Fe}^{-1}$ .

## Experimental Section

**Materials.** Anhydrous solvents were purchased from Kanto Chemicals and used as received. Hexane, toluene, and dichloromethane were distilled over  $\text{CaH}_2$ . THF, 2-methyltetrahydrofuran (2-MeTHF), and diethyl ether were dried over Na and distilled from Na–benzophenone under nitrogen.  $\text{CpCo}(\text{CO})_2$  and  $\text{Ru}(\text{CO})_{12}$  were purchased from Aldrich, 1,2-dibromobenzene, 1,2-benzenedithiol, and  $\text{Me}_3\text{NO}$  were from Tokyo Kasei Chemicals,  $\text{Fe}(\text{CO})_5$  from was from Strem Chemicals, and  $\text{P}^t\text{Bu}_3$  was from Kanto Chemicals.  $[\text{CpCoI}_2(\text{CO})]$ ,<sup>18</sup>  $[\text{CpCoS}_2\text{C}_6\text{H}_4]$  (**1**),<sup>19</sup> poly(*o*-diselenobenzene),<sup>20</sup>  $[\text{CpCoSe}_2\text{C}_6\text{H}_4]_2$  (**2**),<sup>3</sup>  $[\text{Mo}(\text{CO})_3(\text{py})_3]$ ,<sup>21</sup>  $[\text{W}(\text{CO})_3(\text{py})_3]$ ,<sup>21</sup> and  $[\text{Ru}(\text{CO})_3(\text{P}^t\text{Bu}_3)_2]$ <sup>7</sup> were prepared according to the methods in the literature.

**Apparatus.** UV–vis–NIR, IR,  $^1\text{H}$  NMR, EPR, and MALDI-TOF MS spectra were recorded with JASCO V-570 and Hewlett-Packard 8453 UV–vis spectrometers, a JASCO FT/IR-620v spectrometer, JEOL EX270 and Bruker AM 500 spectrometers, a JEOL JES-RE2X spectrometer, and a Shimadzu/KRATOS AXIMA CFR spectrometer, respectively. Cyclic voltammetry and coulometry were carried out with BAS CV 50W and ALS 750A electrochemical analyzers.

**Synthesis.**  $[\{\text{CpCo}(\text{S}_2\text{C}_6\text{H}_4)_2\text{Mo}(\text{CO})_2\}]$  (**3**). All manipulations were carried out under nitrogen or argon. To a stirred solution of **1** (0.106 g, 0.40 mmol) and  $[\text{Mo}(\text{CO})_3(\text{py})_3]$  (0.084 g, 0.20 mmol) in 30 mL ether was added 0.134 mL of  $\text{BF}_3\cdot\text{OEt}_2$  (95.0%, 1.0 mmol) dropwise at room temperature, and the mixture was stirred for 2 h. The solvent was evaporated under vacuum, and the components in the residue were separated by silica gel thin-layer chromatography with toluene/hexane (2:1 v/v) as the eluent. The component on the first band was eluted with toluene and recrystallized from hexane to give 50.1 mg (0.074 mmol, 37%) of brown fine crystals of **3**. Anal. Calcd for  $\text{C}_{24}\text{H}_{18}\text{Co}_2\text{MoO}_2\text{S}_4$ : C, 42.39; H, 2.99; S, 18.85. Found: C, 42.18; H, 2.82; S, 18.59.  $^1\text{H}$  NMR (270 MHz,  $\text{CDCl}_3$ , 25 °C, ppm):  $\delta$  5.15 (s, 5H, Cp), 6.34 (dd,  $J(\text{H,H}) = 5.5, 3.3$  Hz, 2H, Ph), 6.79 (dd, 2H, Ph).

$[\{\text{CpCo}(\text{S}_2\text{C}_6\text{H}_4)_2\text{W}(\text{CO})_2\}]$  (**4**). **1** (0.414 g, 1.57 mmol) and  $[\text{W}(\text{CO})_3(\text{py})_3]$  (0.396 g, 0.784 mmol) were dissolved in 60 mL ether, to which 0.262 mL of  $\text{BF}_3\cdot\text{OEt}_2$  (95.0%, 2.07 mmol) was added, and the solution was refluxed for 45 h. After evaporation of the solvent, the residue was purified by silica gel thin-layer chromatography with toluene/hexane (4:3 v/v) as an eluent. After recrystallization from toluene/hexane (1:1 v/v), **4** was obtained as dark brown crystals at a yield of 67 mg (0.087 mmol, 11%). Anal. Calcd for  $\text{C}_{24}\text{H}_{18}\text{Co}_2\text{O}_2\text{S}_4\text{W}$ : C, 37.52; H, 2.36. Found: C, 37.56; H 2.59.  $^1\text{H}$  NMR (270 MHz,  $\text{CDCl}_3$ , 25 °C, ppm):  $\delta$  4.72 (s, 10H, Cp), 6.17 (dd, 4H,  $J(\text{H,H}) = 5.5, 3.1$  Hz, Ph), 6.97 (dd, 4H, 5.5, 3.1 Hz, Ph).

$[\text{CpCo}(\text{S}_2\text{C}_6\text{H}_4)\text{Fe}(\text{CO})_3]$  (**5**). To a suspension of **1** (0.528 g, 2.0 mmol) and  $\text{Me}_3\text{NO}$  (0.300 g, 4.0 mmol) in toluene (40 mL) was added a toluene solution (10 mL) of  $[\text{Fe}(\text{CO})_5]$  (0.378 g, 2.0 mmol). After the mixture was stirred at room temperature for 2 h,

the volatiles were removed under reduced pressure. The resulting residual was developed by thin-layer chromatography on silica gel with toluene/hexane (1:2 v/v) as an eluent, and the second green fraction was collected. Recrystallization of the green material from pentane gave 0.211 g (0.52 mmol, 26%) of green plate crystals of **5**. Anal. Calcd for  $\text{C}_{14}\text{H}_9\text{CoFeO}_3\text{S}_2$ : C, 41.61; H, 2.24. Found: C, 41.69; H, 2.33.  $^1\text{H}$  NMR (270 MHz,  $\text{CDCl}_3$ , 25 °C, ppm):  $\delta$  4.62 (s, 5H; Cp), 6.04 (dd,  $J(\text{H,H}) = 5.5, 3.1$  Hz, 2H;  $\text{C}_6\text{H}_4$ ), 6.81 (dd,  $J(\text{H,H}) = 5.5, 3.1$  Hz, 2H;  $\text{C}_6\text{H}_4$ ).

$[\text{CpCo}(\text{S}_2\text{C}_6\text{H}_4)\text{Ru}(\text{CO})_2(\text{P}^t\text{Bu}_3)]$  (**6**). The procedure was essentially the same as that for **5**, except that  $[\text{Ru}(\text{CO})_3(\text{P}^t\text{Bu}_3)_2]$  was used instead of  $[\text{Fe}(\text{CO})_5]$ . To a suspension of **1** (0.106 g, 0.4 mmol) and  $\text{Me}_3\text{NO}$  (0.060 g, 0.8 mmol) in toluene (20 mL) was added a toluene solution (10 mL) of  $[\text{Ru}(\text{CO})_3(\text{P}^t\text{Bu}_3)_2]$  (0.118 g, 0.2 mmol). After the mixture was stirred at room temperature for 1 h, the volatiles were removed under reduced pressure. The chromatography was carried out using an alumina (activity III) column with toluene/hexane (1:3 v/v) as an eluent. Yield: 15%. Anal. Calcd for  $\text{C}_{25}\text{H}_{36}\text{CoO}_2\text{PRuS}_2$ : C, 48.15; H, 5.82. Found: C, 48.34; H, 5.83.  $^1\text{H}$  NMR (270 MHz,  $\text{CDCl}_3$ , 25 °C, ppm):  $\delta$  1.28 (d, 27H;  $\text{P}^t\text{Bu}_3$ ), 4.96 (s, 5H; Cp), 6.20 (dd,  $J(\text{H,H}) = 5.5, 3.3$  Hz, 2H;  $\text{C}_6\text{H}_4$ ), 7.04 (dd,  $J(\text{H,H}) = 5.5, 3.3$  Hz, 2H;  $\text{C}_6\text{H}_4$ ).

$[\{\text{CpCo}(\text{Se}_2\text{C}_6\text{H}_4)_2\text{Mo}(\text{CO})_2\}]$  (**7**). **Method A.** A mixture of **2** (0.072 g, 0.10 mmol) and  $[\text{Mo}(\text{CO})_3(\text{py})_3]$  (0.042 g, 0.10 mmol) in 20 mL of ether was added to 0.033 mL of  $\text{BF}_3\cdot\text{OEt}_2$  (95.0%, 0.30 mmol), followed by stirring for 3 h at room temperature. The solvent was evaporated under vacuum, and the components in the residue were separated by alumina column chromatography with dichloromethane/hexane (1:1 v/v) as an eluent. Yield: 0.024 g (0.027 mmol, 28%).

**Method B.** A mixture of **2** (0.072 g, 0.10 mmol) and  $[\text{Mo}(\text{CO})_3(\text{py})_3]$  (0.042 g, 0.10 mmol) in 40 mL of dichloromethane solution was stirred for 90 h at room temperature. The solvent was evaporated under vacuum, and the components in the residue were separated by alumina column chromatography with dichloromethane/hexane (1:1 v/v) as an eluent. Yield: 0.083 g (0.10 mmol, 95%). Anal. Calcd for  $\text{C}_{24}\text{H}_{18}\text{Co}_2\text{MoO}_2\text{Se}_4\cdot\text{H}_2\text{O}$ : C, 32.53; H, 2.28. Found: C, 32.61; H, 2.24.  $^1\text{H}$  NMR (270 MHz,  $\text{CDCl}_3$ , 25 °C, ppm):  $\delta$  5.09 (s, 10H, Cp), 6.48 (dd, 4H,  $J(\text{H,H}) = 5.5, 3.2$  Hz, Ph), 6.95 (dd, 4H, 5.5, 3.2 Hz, Ph). MALDI-TOF MS ( $m/z$ ): 811 ( $M - 2(\text{CO})^+$ ).

$[\{\text{CpCo}(\text{Se}_2\text{C}_6\text{H}_4)_2(\text{Se}_2\text{C}_6\text{H}_4)\text{W}(\text{CO})_2\}]$  (**8**). **Method A.** To a mixture of **2** (0.045 g, 0.063 mmol) and  $[\text{W}(\text{CO})_3(\text{py})_3]$  (0.032 g, 0.063 mmol) in 20 mL of ether was added 0.070 mL of  $\text{BF}_3\cdot\text{OEt}_2$  (95.0%, 0.63 mmol), followed by stirring for 2 h at reflux. The solvent was evaporated under vacuum, and the components in the residue were separated by silica gel column chromatography with toluene/hexane (1:1 v/v) as an eluent. Yield: 0.003 g (0.0035 mmol, 7%). Anal. Calcd for  $\text{C}_{19}\text{H}_{13}\text{CoO}_2\text{Se}_4\text{W}\cdot 2\text{H}_2\text{O}$ : C, 26.29, H, 1.97. Found: C, 26.36, H, 2.23.  $^1\text{H}$  NMR (270 MHz,  $\text{CDCl}_3$ , 25 °C, ppm):  $\delta$  5.17 (s, 5H, Cp), 6.86 (dd, 2H,  $J(\text{H,H}) = 5.5, 3.0$  Hz, Ph), 7.29 (dd, 2H, 6.1, 3.2 Hz, Ph), 7.50 (dd, 2H, 5.5, 3.0 Hz, Ph), 8.38 (dd, 2H, 6.1, 3.2 Hz, Ph). MALDI-TOF MS ( $m/z$ ): 778 ( $M - 2(\text{CO})^+$ ).

**Method B.** To a mixture of **2** (0.036 g, 0.050 mmol) and  $[\text{W}(\text{CO})_3(\text{py})_3]$  (0.025 g, 0.050 mmol) in 20 mL of toluene was added 0.034 mL of  $\text{BF}_3\cdot\text{OEt}_2$  (95.0%, 0.25 mmol), followed by stirring for 2 h at room temperature. The product in the filtrate was chromatographed on an alumina column (activity: II–III) with toluene/hexane (1:2 v/v). Compound **8** was obtained from the second band, 0.014 g (0.016 mmol, 33%). The compound obtained from the first band could not be purified satisfactorily because it was very sensitive to air and water and decomposed to give **4** even

(18) (a) King, R. B. *Inorg. Chem.* **1966**, 5, 82. (b) Heck, R. F. *Inorg. Chem.* **1965**, 4, 855.

(19) Heck, R. F. *Inorg. Chem.* **1968**, 7, 8.

(20) Sandman, D. J. *Inorg. Chem.* **1987**, 26, 1664.

(21) Hieber, W.; Muhlbauer, F. Z. *Anorg. Allg. Chem.* **1935**, 221, 337.

at room temperature in organic solution. The spectral data obtained were as follows.  $^1\text{H}$  NMR (270 MHz,  $\text{CDCl}_3$ , 25 °C, ppm):  $\delta$  5.19 (s, 10H, Cp), 6.72 (dd, 4H,  $J(\text{H,H}) = 5.5, 3.1$  Hz, Ph), 7.44 (dd, 4H, Ph). IR (KBr disk):  $\tilde{\nu} = 2033, 1957, 1876$   $\text{cm}^{-1}$  (CO). UV (toluene solution):  $\lambda_{\text{max}} = 449$  nm ( $\epsilon = 9139$   $\text{mol}^{-1} \text{dm}^3 \text{cm}^{-1}$ ). These data are similar to those of **7**, indicating strongly that it is a trinuclear  $\text{Co}_2\text{W}$  complex with a structure comparable to **7**.

**Single-Crystal Structure Determination.** Suitable single crystals of **3–5**, **7**, and **8** were grown. The crystals of **3–5** were sealed in a glass capillary, whereas those of **7** and **8** were mounted in a loop. The data for **3–5** were collected with a Rigaku AFC-7R diffractometer equipped with a rotating-anode X-ray generator. The data for **7** and **8** were collected with a Rigaku AFC8 diffractometer with the Rigaku Mercury CCD system. The X-ray used was graphite-monochromated Mo  $\text{K}\alpha$  radiation ( $\lambda = 0.7107$  Å). Structure solution and refinement were performed with the teXsan software package (Molecular Structure Corp.) for **3–5** and with the Crystal Structure ver 3.5.1 software package (Rigaku) for **7** and **8**. Selected crystallographic data and experimental details are listed in Table 1.

**Electrochemical Measurements.** A glassy carbon rod (diameter 5 mm; Tokai Carbon GC-20) was embedded in Pyrex glass, and the cross section was used as a working electrode for cyclic voltammetry. Cyclic voltammetry measurements were carried out in a standard one-compartment cell equipped with a platinum-wire counter electrode and an  $\text{Ag}/\text{Ag}^+$  reference electrode under argon. Coulometry was carried out in a three-compartment cell equipped

with a carbon rod (5 mm i.d.  $\times$  2 cm) working electrode, a platinum-wire counter electrode, and an  $\text{Ag}/\text{Ag}^+$  reference electrode under argon. Cyclic voltammograms were simulated using the DigiSim ver 3 software package.

**Spectroscopy of the Reduction Products.** A THF solution of a complex and Na mirror was prepared in a tube to which was attached a UV cell and/or a EPR sample tube. The solution was cooled with liquid  $\text{N}_2$  and sealed under vacuum, as described in a reference.<sup>14c</sup> The solution was reduced stepwise, and UV spectra and/or EPR spectra were measured.

**ZINDO Calculations.** The molecular orbital calculation for **5**, on the basis of the structure obtained by X-ray analysis, was carried out using the ZINDO/S method, using the default parameters of the software HyperChem (Hypercube Inc.).

**Acknowledgment.** This work was supported by Grants-in-Aid for Scientific Research (Nos. 16074204 (area 434) and 17205007) from the Ministry of Culture, Education, Science, Sports, and Technology of Japan, by a grant from The 21st Century COE Program for Frontiers in Fundamental Chemistry, and by CREST, JST, Japan.

**Supporting Information Available:** X-ray crystallographic data in CIF format. This material is available free of charge via the Internet at <http://pubs.acs.org>.

IC0513282